SOLAR TRACKER FAILURE DETECTION OF SONDA PETROLINA SOLARIMETRIC STATION

Lucas Emanuel A. Barboza – lucas.barboza@ufpe.br
Solluan da Silva Marçal Nunes
Adriana Ellen de Farias
Emilly Raquel Oliveira da Silva
Lucas André Paes e Silva
Olga C. Vilela
Andre Felippe Vieira da Cunha
Federal University of Pernambuco, Renewable Energy Center

Abstract. *This document presents a method to infer solar tracker probabilistic reliability indices from Solarimetric Stations measurements. The methodology collects global, beam, and diffuse irradiances data. It establishes a usual criterion to determine solar tracker failure days, based on the premise that when the tracker stocks, pyrheliometer and shadow ball do not move, implying that global irradiance is almost equal to the diffuse along the day, and beam irradiance is very low. The failures are reanalyzed, and a two-parameter Weibull distribution fits the reliability and failure rate curves considering the monotonic behavior in the operation times. The procedure was applied for the SONDA solarimetric station in Petrolina, state of Pernambuco, Brazil. Results show a mean time between failures lower than 18 months, indicating that an annual maintenance rate is appropriate to avoid this type of failure.*

Keywords: *Solar Tracker, Failure Detection, Probabilistic Reliability Indices.*

1. INTRODUCTION

Solarimetric stations measure local solar irradiation to estimate local solar energy resources. The stations generally use a pyranometer, which accepts radiation from the entire hemisphere, and a pyrheliometer, which accepts radiation from approximately one direction (more precisely from a cone of 2.8° half-angle) (Rabl, 1985). A pyranometer measures the hemispherical (global) irradiance; a pyrheliometer pointing to the Sun measures beam irradiance; a pyranometer with a shadow ball shadowing the Sun's direct irradiation measures diffuse irradiation. For this purpose, solarimetric stations also have a solar tracker moving pyrheliometer and shadow ball. Fig. 1 shows the SONDA Petrolina solar tracker with two pyranometers, one pyrheliometer, and shadow balls.

Figure 1 - Petrolina SONDA Solarimetric Station solar tracker, with two pyranometers, one pyrheliometer, and shadow ball equipment.
Source: SONDA (2007).

In this sense, one of the most relevant solarimetric station operational problems is solar tracker failures (Brennand and Paula, 2018). Gonzalez-Cabrera *et al.* (2018) reported that 3 of 10 solarimetric stations in Mexico experienced issues with their solar trackers over a two-year operational period. Similarly, Relva *et al.* (2017) addressed problems with solar trackers at two stations in the state of São Paulo, Brazil, where the trackers had to be deactivated for maintenance in another country. The authors affirm that solar tracker misalignments can occur mainly in stations with inadequate maintenance and monitoring.

The solar tracker failure in solarimetric stations results in a wrong solar irradiance measurement. To mitigate this issue, several authors have incorporated data quality assessment procedures to verify the tracker status, like Silva *et al*. (2014), Linhares *et al.* (2019), and Miranda *et al*. (2022), developing procedures that utilize coefficients, such as Kd and Kt. These researchers established coefficient limits for tracker operation, which vary across the studies. Nevertheless, a common hypothesis adopted in these studies is based on irradiance data on a clear sky day to ascertain the tracker functionality. For clear sky days with a significative amount of measurements, if the global irradiance closely matches the diffuse irradiance and the beam irradiance remains significantly low throughout the day, it indicates a non-operational tracker.

Despite these findings, there is a lack of studies in the literature that specifically investigate the reliability of solar trackers in solarimetric stations. Therefore, based on standard tracker-off models in literature, this work aims to detect solar tracker failure days in a solarimetric station localized in Petrolina (state of Pernambuco), a city in Brazil's northeast. The detection methodology presented in this work uses hemispherical, beam, and diffuse irradiances measurements to determine daily tracking system failures. Then, the study will present the Petrolina solar tracker solarimetric station Reliability and Failure Rate Curves using the failure days detected by the methodology.

Probabilistic indices, such as the Reliability Curve and Failure Rate Function, are important in applying preventive maintenance optimization models using reliability probabilistic metrics (Ghosh and Roy, 2009; Vílchez-Torres *et al.*, 2020). These models associate the reliability distributions of specific equipment with cost functions, thereby optimizing maintenance schedules based on a reliability-centred maintenance calendar (Guo *et al.*, 2016). This approach not only boosts the efficiency of maintenance operations but also substantially cuts costs, as it employs distribution metrics to prevent failures proactively.

2. MATERIALS AND METHODS

This work uses the data from the SONDA solarimetric station in Petrolina, state of Pernambuco, Brazil. The SONDA project, initiated by Brazil's National Institute of Space Research (INPE), is a data network designed to enhance the database of solar and wind energy resources in Brazil by implementing physical infrastructure and human resources (SONDA, 2019). Its purpose is to support the country's growth and improvement of renewable energy utilization. From the Petrolina station, global (I_h), beam (I_b), and diffuse (I_d) irradiances data (in W/m^2) were collected. The data start on 2004-07-01 00:00:00 and finish on 2019-02-28 23:58:59, at a timestep by one minute.

First, the GMT data needed to be adjusted to GMT -3 because it is in GMT 0. Second, the methodology only uses data between sunrise and sunset; in this sense, one common practice is to get data with zenith angle (θ_z) less than 87° (Petribú *et al.*, 2017). Then, we applied quality assurance procedures to the data. Two types of data quality tests are applied: global and local.

The global tests evaluate chronological sorting, timestamps duplication, non-uniform timestamps, and time gaps (Petribú *et al.*, 2017). The chronological sorting test sorts the irradiances by the dates. The second test analyses the existence of duplicate timestamps. If there are duplicates, the duplicate sample values are analyzed. If they are the same, the test eliminates duplicates, keeping one sample value associated with that duplicate timestamp; if not, the duplicate timestamp sample receives not-a-number (NAN), and the duplicates are eliminated. Next, the non-uniform test analyses timestamps that do not follow the timestep. For example, consider the timestamps 2023-11-30 12:00, 2023-11-30 12:58, and 2023-11-30 14:00 at a timestep by one hour. In the non-uniform timestamps procedure, the 2023-11-30 12:58 timestamp will be corrected to 2023-11-30 13:00. Finally, the time gaps test searches for gaps in timestamps; in other words, if there are missing timestamps. Then, the data receive the absent timestamps, which samples are set as NAN.

The local test applies the recommended BRSN (Baseline Surface Radiation Network) physical limits shown in Eqs. (1), (2), and (3) (Long and Dutton, 2010)

$$-4 \leq I_h \leq I_{0eff} \cdot 1{,}5 \cdot \cos^{1,2}(\theta_z) + 100 \tag{1}$$

$$-4 \leq I_b \leq I_{0eff} \tag{2}$$

$$-4 \leq I_d \leq I_{0eff} \cdot 0.95 \cdot \cos^{1,2}(\theta_z) + 50 \tag{3}$$

where θ_z *is* the zenith angle and I_{0eff} is the effective solar constant (Rabl, 1985).

The next step is to detect daily failures in the solarimetric station solar tracker system. Based on the previous literature about tracker-off, Miranda *et al.* (2022) show that, for clear sky days, when the tracker fails in a large part of

the day, the global irradiance is approximately equal to diffuse, while beam irradiance is very low. It means that the pyrheliometer and shadow ball get stuck (the tracker system does not move). This phenomenon can be seen in Fig. 2: on August 27th, 2007, the day was a clear sky day, the diffuse and global irradiances were almost equal, and beam irradiance was very low.

Because of this, the method adopted four simultaneous criteria to set a day as a failure:

1. The I_h, I_b, and I_d daily series has simultaneously at least 60% of the samples valid (not NAN);
2. The day is a clear sky day;
3. At least 50% of daily sample I_h is equal to I_d with a maximum/minimum band of 10%; and
4. At least, 50% of daily sample I_b is less than $50\ W/m^2$

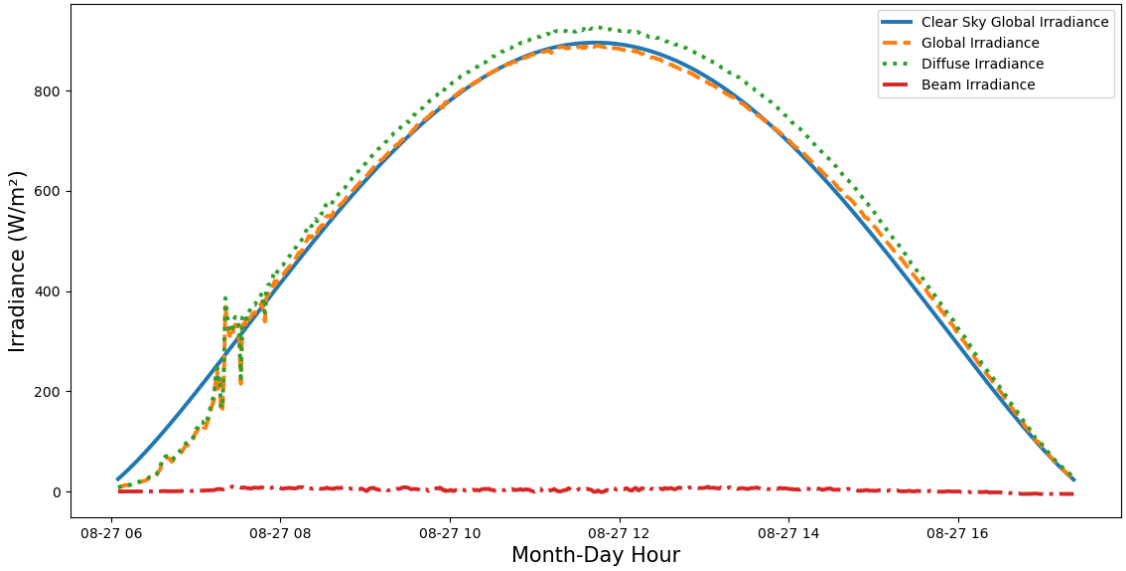

Figure 2 – Clear Sky Global Irradiance and Measured Irradiances on August 27th, 2007

The clear sky days identification uses Long and Ackerman (2000) model. This model is a power law ruling the zenith and the clear sky global irradiance ($I_{h,CC}$) by the A and B coefficients, as seen in Eq. (4). These coefficients are daily fitted minimizing mean square error by a Levenberg-Marquardt optimization method (More, 1977). After the curve fit, the daily I_h series is compared with $I_{h,CC}$ by Pearson correlation − days with a correlation higher than 0.96 are classified as clear sky. The threshold of 0.96 was determined through a sensibility analysis and has proven to be an effective limit for distinguishing clear sky days.

$$I_{h,CC} = \text{A}\cos^{B}(\theta_z) \quad (4)$$

The failure data is reanalyzed two rounds after the daily failure detection using the previous criteria. In the first round, the adopted assumption is that the failures continue until an indication of the tracker properly functioning. Therefore, if a day is classified as failure, these subsequent days are classified as failure, too, until a day when the first and second criteria are true and three or four are false. This assumption is based on the fact that a solar tracker is still in a state of failure until a repair occurs, which is indicated by getting false in the third or fourth criteria on a valid clear sky day.

The second round of reanalysis involves a more nuanced approach. Here, any short periods of functioning days (less than 3) sandwiched between longer periods of failure days (at least fifteen days) are also classified as failures. This assumption is based on the rationale that brief periods of apparent functionality within prolonged failure periods may not truly represent a return to normal operation but rather temporary fluctuations or anomalies. Thus, for this analysis, they are treated as part of the ongoing failure period.

Tab. 1 illustrates the failure detection procedures previously described. The first column displays the timestamp, while the second, third, fourth, and fifth columns indicate whether the corresponding timestamp meets the criteria. The Class column represents a failure if all four criteria are met simultaneously. The final two columns represent the two rounds of post-processing applied to the initial data classifications.

The day 2023-01-01 received a failure class flag because it achieved all four criteria. 2023-01-02 and 2023-01-03 received functioning classes based on the same criteria; nevertheless, after the first reanalysis, they received failure classes because only in 2023-01-01 the third criterion is false for a valid clear sky day (first and second criteria met

represent valid clear sky days), indicating that the tracker system has been repaired. 2023-01-04 does not have a classification because it is a day with I_h, I_b, and I_d daily series not having simultaneously at least 60% of the samples not NAN values; however, it was set as a failure because the class before was a failure. This last procedure is used for all days the first criterion is not met. Finally, 2023-02-04 represents a timestamp classified as a failure after the second reanalyze because there are many failure days (at least fifteen) before and after that, and it was an isolated timestamp initially classified as functional.

Table 1 - Example of Solarimetric Station Solar Tracker System Failures Detection Steps

TIME-STAMP	1ST CRITERION MET	2ND CRITERION MET	3RD CRITERION MET	4TH CRITERION MET	CLASS	1ST REANA-LYZED CLASS	2ST REANALY-ZED CLASS
2023-01-01	Yes	Yes	Yes	Yes	Failure	Failure	Failure
2023-01-02	Yes	No	Yes	Yes	Function	Failure	Failure
2023-01-03	Yes	No	Yes	Yes	Function	Failure	Failure
2023-01-04	No	–	–	–	–	Failure	Failure
2023-01-05	Yes	Yes	No	Yes	Function	Function	Function
(...)							
2023-02-01	Yes	Yes	Yes	Yes	Failure	Failure	Failure
2023-02-02	Yes	Yes	Yes	Yes	Failure	Failure	Failure
2023-02-03	Yes	Yes	Yes	Yes	Failure	Failure	Failure
2023-02-04	Yes	Yes	No	No	Function	Function	Failure
2023-02-05	Yes	Yes	Yes	Yes	Failure	Failure	Failure
2023-02-06	Yes	Yes	Yes	Yes	Failure	Failure	Failure

This methodology gets operation and failure times analyzing consecutive functioning days and consecutive failure days, respectively. The alternating operation and failure times represent a renewal cycle. It can be seen in Fig. 3. One way to model this process is by an Ordinary Renewal Process (ORP). In an ORP, the renewal cycle is approximately the operation time because failure time (or repair time) represents a small part of the cycle (Wang and Yang, 2012). Then, the operation time conjunct is used to model the probabilistic reliability indices.

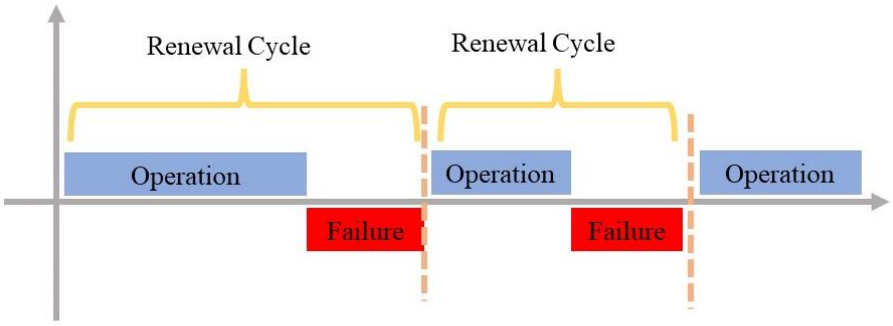

Figure 3 - Renewal Process Schema

The probabilistic reliability indices study time to failure random variable **T**. $F(t) = P\{\boldsymbol{T} \leq t\}$ is the cumulative distribution function (CDF), and $f(t)$ is the probability density function (PDF). The main probabilistic reliability indices are the Reliability Function ($R(t)$) and Failure Rate Function ($\lambda(t)$), whose definition is presented in Eqs. (5) and (6) (Lewis *et al.*, 1994). $R(t)$ indicates a probability that the system is functioning until the time t. In its

turn, $\lambda(t)$, also known as the bathtub curve, analyzes the failure types, showing if the system has more early, random, or aging failures. Finally, the mean time to failure (MTTF) is presented in Eq. (7).

$$R(t) = 1 - F(t) \tag{5}$$

$$\lambda(t) = \frac{f(t)}{R(t)} \tag{6}$$

$$MTTF = \int_0^\infty R(t)dt \tag{7}$$

One common practice is using a two-parameter Weibull distribution to monotonic curve fits because Weibull distribution can adjust various failure rate behaviors (Lewis et al., 1994). The Weibull two parameters are scale factor (ε) and shape factor (τ). $\tau < 1$ represents systems with a prevalence of early failures, $\tau = 1$ systems with predominant random failures, $\tau > 1$ aging failures (Lewis *et al.*, 1994). Eqs. (8), (9), and (10) show CDF, Reliability Function, and Failure Rate Function for a two-parameter Weibull distribution.

$$F(t) = 1 - \exp\left[-\left(\frac{t}{\varepsilon}\right)^{\tau}\right] \tag{8}$$

$$R(t) = \exp\left[-\left(\frac{t}{\varepsilon}\right)^{\tau}\right] \tag{9}$$

$$\lambda(t) = \frac{\tau}{\varepsilon}\left(\frac{t}{\varepsilon}\right)^{\tau-1} \tag{10}$$

Weibull CDF can be linearized. Eq. (11) shows two-parameter Weibull CDF in linear format $Y = aX + b$. The angular coefficient a is τ, while linear coefficient b is $-\tau \ln \varepsilon$. The Y and X transformations are shown in Eqs. (12) and (13), respectively. Finally, Eqs. (14) and (15) demonstrate how to calculate τ and ϵ by minimizing the least square error.

$$\ln\left[\ln\left(\frac{1}{1 - F(t)}\right)\right] = \tau \ln t - \tau \ln \varepsilon \tag{11}$$

$$Y_i = \ln\left[\ln\left(\frac{1}{1 - F(t_i)}\right)\right] \tag{12}$$

$$X_i = \ln t_i \tag{13}$$

$$\tau = \frac{n\sum_{i=1}^{n}(Y_i X_i) - \sum_{i=1}^{n}(Y_i)\sum_{i=1}^{n}(X_i)}{n\sum_{i=1}^{n}(X_i) - \left(\sum_{i=1}^{n}(X_i)\right)^2} \tag{14}$$

$$\varepsilon = \exp\left(-\frac{\sum_{i=1}^{n}(Y_i) - \tau\sum_{i=1}^{n}(X_i)}{\tau n}\right) \tag{15}$$

The conjunct of pairs $(t, F(t))$ to two-parameters Weibull curve fit is necessary, but the solarimetric station solar tracker failure detection only delivers operation times. Therefore, it is necessary to have a way to estimate the cumulative probabilities $F(t)$ associated with each operational time t. A common practice is to adjust $F(t)$ using the median rank (O'Connor and Kleyner, 2012). The median rank sorts the operation times by length and estimates the cumulative probability by a relationship that uses the beta function (Jacquelin, 1993). The rank formula of the median is

complex, and that is why using approximations, one of them presented in Eq. (16), called Bernard approximation, which i_{t_i} represents the operational time order, and n the samples quantities (O'Connor and Kleyner, 2012).

$$\hat{F}_i = \frac{i_{t_i} - 0{,}3}{n + 0{,}4} \tag{16}$$

In the operational times of the solar tracker at the Petrolina SONDA solarimetric station, there is a specific period referred to as suspended time, representing right-censored data. The concept of censored data pertains to observations where the exact occurrence of the event of interest, in this case, a failure, is not precisely known. Nevertheless, it is known that the event has yet to occur up to the last data timestamp. Suspended items are not plotted as data points on the graph, but their existence affects the ranks of the remaining data points (O'Connor and Kleyner, 2012). In other words, right-censored data do not have an i_{t_i}; however, the i_{t_i} of the other operating times are affected by it. Eqs. (17) and (18) show how to readjust i_{t_i} values for a conjunct with right-censored data. In these, it is possible to see that the suspended data do not have an i_{t_i}, but its existence affects the other data's i_{t_i} value.

$$N_{t_i} = \frac{(n+1) - i_{t_{i-1}}}{1 + (n - \ number\ of\ preceding\ items)} \tag{17}$$

$$i_{t_i} = i_{t_{i-1}} + \ N_{t_i} \tag{18}$$

3. RESULTS

Tab. 2 displays the results of the quality test conducted for the Petrolina SONDA Solarimetric Station. The table details the initial total sample count, 7222602, and enumerates the quantity of samples identified in each test. Additionally, it provides the percentage that each test's sample count represents of the initial total sample count. Non-uniform timestamps are the major detection with 14.14%, which is not a big deal because this procedure represents only date corrections. Time gaps represent 6.78% of the sample total, a value less than 10%, which is the acceptable limit. Less than 1% of the total is out of BRSN physical limits for irradiance measurements.

Table 2 - Quality Tests Results for the Petrolina SONDA Solarimetric Station

QUALITY TEST		SAMPLES QUANTITIES	PERCENTAGE
TYPE	SPECIFIC		Initial Total: 7222602
Global	Duplicates timestamps	10	0.00%
	Non-uniform timestamps	1021440	14.14%
	Time Gaps	490038	6.78%
Local	BRSN I_h limits	3952	0.00%
	BRSN I_b limits	28217	0.39%
	BRSN I_d limits	4375	0.00%
	TOTAL	1548032	21.43%

Tab. 3 presents operational and repair times sorted by operational times length. The first four columns offer information about the renewal cycle, including the initial timestamp, the length of operation time and repair (or failure) time in days, and an indication of whether there is a suspended time or not. The repair time mean of 36.72 days divided by the renewal cycle time (operation plus repair) mean of 424.91 days results in 8.64%, excluding suspended data, which implies that the repair time represents a small part of cycles. As a result, an Ordinary Renewal Process can be feasibly applied. Operation times cumulative probabilistic approximation by median rank $\hat{F}_i$ is in Table 3 last column. The 2017-04-18 timestamp is a suspended time, and it does not have an i_{t_i} value and consequently does not have a rank

$\hat{F}_i$, as seen. Nevertheless, this suspended time affects the other ranks, specifically 2004-07-01 and 2012-03-09 timestamps rank.

Table 3 - Operational and Reparation Times Summary and Adjusted Ranks Calculation by Bernard's Approximation of Median Rank

RENEWAL CYCLE START TIMESTAMP	OPERATIONAL TIME (days)	REPAIR TIME (days)	SUSPENDED DATA?	N_{t_i}	i_{t_i}	$\hat{F}_i$
2008-09-28	13	21	No	1.00	1.00	0.06
2008-11-01	35	13	No	1.00	2.00	0.14
2007-11-21	69	25	No	1.00	3.00	0.22
2010-08-06	88	18	No	1.00	4.00	0.30
2016-11-18	92	59	No	1.00	5.00	0.38
2008-12-19	182	78	No	1.00	6.00	0.46
2008-02-23	213	5	No	1.00	7.00	0.54
2009-09-05	332	3	No	1.00	8.00	0.62
2010-11-20	467	8	No	1.00	9.00	0.70
2017-04-18	682	–	Yes	–	–	–
2004-07-01	1152	86	No	1.33	10.33	0.81
2012-03-09	1627	21	No	1.33	11.67	0.92

Fig. 4 shows the fit of the two-parameter Weibull CDF distribution curve. The axes represent the linearization of Weibull distribution with $Y = \ln\left[\ln\left(\frac{1}{1-F}\right)\right]$ and $X = \ln t$. The points plotted are the cumulative probability estimate by Bernard's approximation of median rank. The data has a monotonic behavior, as can seen by the linear tendency of the points, which implies that the two-parameter Weibull CDF can represent it. The fit has a high determination coefficient (R^2) of approximately 0.97, which is a good adjustment. By this fit, the scale factor (ε) and shape factor (τ) are 396.38 and 0.75, respectively, as shown in Fig. 4. The failures have a behavior predominant of infant failures because τ is less than one.

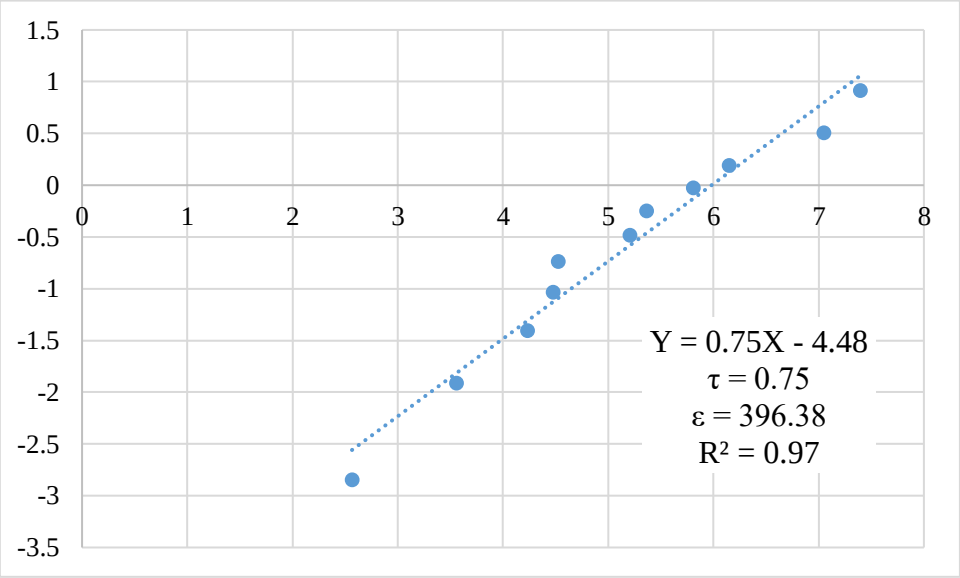

Figure 4 - Two-parameter Weibull CDF distribution curve fit of SONDA Petrolina solar tracker operation times, with $Y = \ln\left[\ln\left(\frac{1}{1-F(t)}\right)\right]$ and $X = \ln t$

Fig. 5 and Fig. 6 present the Reliability Curve and Failure Rate Function of the SONDA Petrolina solar tracker, respectively. After one year, the system's reliability is less than 50%. Because of that, the failure rate exhibits its highest values at the onset of operation. Notably, during the initial 200 days, there is a rapid decrease in the failure rate. Subsequently, this rate of decrease diminishes considerably.

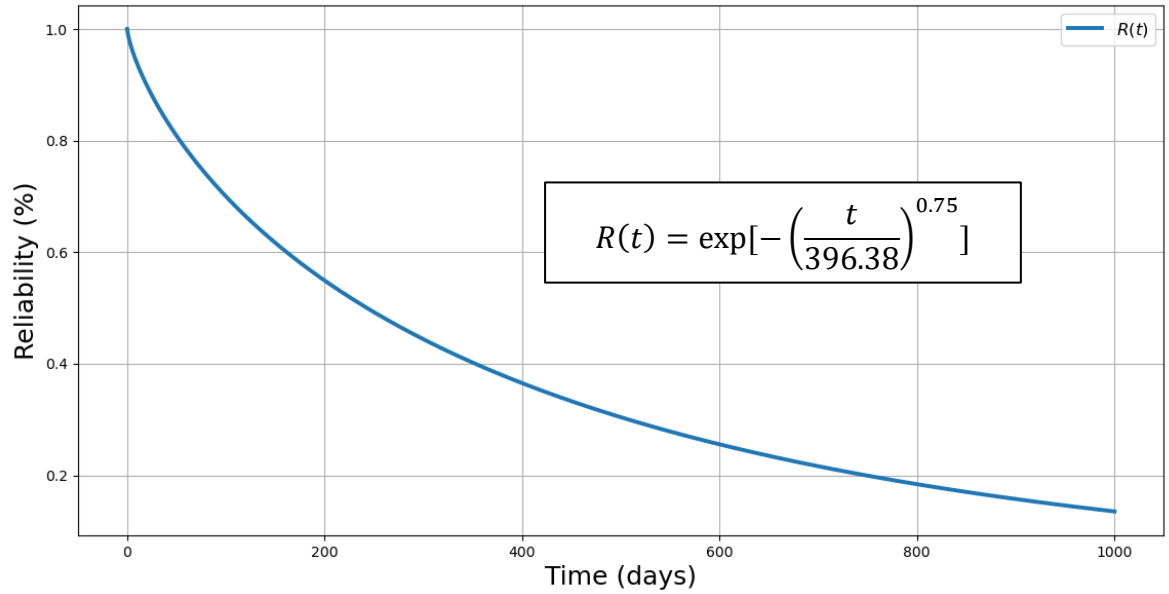

Figure 5 - Reliability Curve of SONDA Petrolina solar tracker

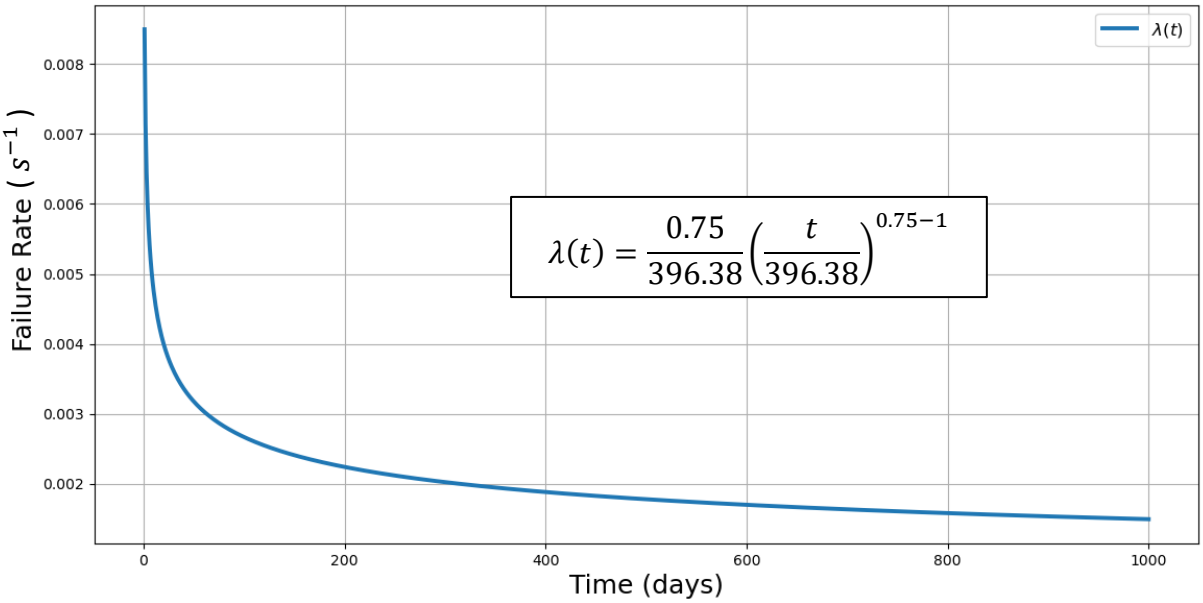

Figure 6 - Failure Rate Curve of SONDA Petrolina solar tracker

Finally, using Eq. (7), the Mean Time to Failure (MTTF) is calculated to be 472.67 days, signifying that the interval between failures exceeds one year in the mean. This MTTF suggests that annual maintenance is viable for the solar tracker at the SONDA Petrolina solarimetric station. This finding is noteworthy as the solar tracker manufacturer recommends maintenance twice yearly (Kipp & Zonen, 2005), suggesting that maintenance could be done with a higher time interval (considering the data analyzed). Future work could employ probabilistic reliability indices derived from this methodology in conjunction with cost functions to schedule maintenance and minimize costs precisely.

4. CONCLUSIONS

This work aims to build a methodology for detecting failure days of the SONDA Petrolina solarimetric station solar tracker to infer the system's reliability and failure rate curves. Based on previous literature, the detection methodology utilizes the irradiances measures associated with certain criteria. The post-processing of the results was especially important for the detection, which allowed for enlarging the failure times based on the premise that the tracker only gets repaired if the data explicitly shows that. After that, the reliability probabilistic indices are inferred by curve fit, paying special attention to the use of suspended data. By the end, the MTTF results in 472.67 days, one value that implies that annual maintenance for the solar trackers could be a good practice despite the twice-yearly maintenance recommended by the manufacturer. Future works could employ this methodology associated with cost functions to schedule maintenance with minimal costs.

REFERÊNCIAS

Brennand, L.J. de P., Paula, J.G.S. de, 2018. Avaliação da qualidade de dados observacionais de vento e radiação solar. UFPE, Recife.

Ghosh, D., Roy, S., 2009. Maintenance optimization using probabilistic cost-benefit analysis. J Loss Prev Process Ind 22, 403–407. https://doi.org/10.1016/j.jlp.2009.01.007

Gonzalez-Cabrera, A.E., Riveros-Rosas, D., Valdes-Barrón, M.G., Bonifaz-Alfonzo, R., Velasco-Herrera, V.M., Estevez-Perez, H.R., Carabali, G., 2018. New reference solarimetric network for Mexico, in: AIP Conference Proceedings. American Institute of Physics Inc. https://doi.org/10.1063/1.5067192

Guo, J., Li, Z., Wolf, J., 2016. Reliability centered preventive maintenance optimization for aircraft indicators, in: Proceedings - Annual Reliability and Maintainability Symposium. Institute of Electrical and Electronics Engineers Inc. https://doi.org/10.1109/RAMS.2016.7448068

Jacquelin, J., 1993. A Reliable Algorithm for the Exact Median Rank Function. IEEE Transactions on Electrical 28, 168–171.

Kipp & Zonen, 2005. Instruction Manual 2 AP 2-Axis Sun Tracker / Positioner Gear Drive.

Lewis, E.E., Wiley, J., York, N., Brisbane, C., Singapore, T., 1994. Introduction to Reliability Engineering, 2nd ed. John Wiley & Sons, INc.

Linhares, A.L., Luiz, ;, Galvão, C.R., Morales Udaeta, M.E., Luis, A., Gimenes, V., 2019. Analysis of the Approaches Seeking Quality in Anemometric and Solarimetric Data for Energy Production. Journal of Multidisciplinary Engineering Science and Technology (JMEST) 6, 2458–9403.

Long, C.N., Ackerman, T.P., 2000. Identification of clear skies from broadband pyranometer measurements and calculation of downwelling shortwave cloud effects. Journal of Geophysical Research Atmospheres 105, 15609–15626. https://doi.org/10.1029/2000JD900077

Long, C.N., Dutton, E.G., 2010. BSRN recommended QC tests.

Miranda, D., Petribú, L., Galdino, J., Furtado, J.V., Barboza, L., Vilela, O., Costa, A., Gomes, E., Pereira, A., Jatobá, E., Neto, A.C., Filho, J.B., 2022. Quality Assurance Procedure for Solar Radiation at Minute Resolution, in: EuroSun2022. https://doi.org/10.18086/eurosun.2022.15.04

More, J.J., 1977. The Levenberg-Marquardt algorithm: Implementation and theory, in: Numerical Analysis: Proceedings of the Biennial Conference Held at Dundee. pp. 105–116. https://doi.org/10.1007/BFb0067700

O'Connor, P.D.T., Kleyner, A., 2012. Practical Reliability Engineering, 5th ed. John Wiley & Sons,.

Petribú, L., Sabino, E., Barros, H., Costa, A., Barbosa, E., Vilela, O., Luiz Freire, A., 2017. PROCEDIMENTO OBJETIVO PARA A GARANTIA DE QUALIDADE DE DADOS DE RADIAÇÃO SOLAR 21, 11–67.

Rabl, A., 1985. Active Solar Collectors and Their Applications, 1st ed. Oxford University Press, Inc, New York.

Relva, S., Edgar Morales Udaeta, M., Silva, V., Gimenes, A., Gomes, S., Edgar Morales, M., Oliveira, V., Luiz Veiga, A., Claudio Ribeiro, L., 2017. Comprehensive Analysis of Solarimetry Elements for Primar Energy Forecasting Methodologies Related to Photovoltaic Power Plants, in: 33rd European Photovoltaic Solar Energy Conference and Exhibition. pp. 2463–2469. https://doi.org/10.4229/EUPVSEC20172017-6BV.3.10

Silva, P.E.D. da, Pereira, E., Martins, F., Pereira, S., 2014. Quality Control of Solar Radiation Data within Sonda Network in Brazil: Preliminary Results, in: EuroSun ISES Conference Proceedings. International Solar Energy Society (ISES). https://doi.org/10.18086/eurosun.2014.08.04

SONDA, 2019. SONDA - Estação Petrolina [WWW Document]. URL http://sonda.ccst.inpe.br/basedados/petrolina.html (accessed 12.6.23).

SONDA, 2007. SONDA - Fotografia da Estação de Petrolina [WWW Document]. URL http://sonda.ccst.inpe.br/fotos/petrolina_fotos_2007.html (accessed 12.6.23).

Vílchez-Torres, M.K., Oblitas-Cruz, J.F., Castro-Silupu, W.M., 2020. Optimization of the replacement time for critical repairable components. DYNA (Colombia) 87, 93–99. https://doi.org/10.15446/DYNA.V87N214.84509

Wang, Z.M., Yang, J.G., 2012. Numerical method for Weibull generalized renewal process and its applications in reliability analysis of NC machine tools. Comput Ind Eng 63, 1128–1134. https://doi.org/10.1016/j.cie.2012.06.019